Am J Physiol Regul Integr Comp Physiol 294: R1752–R1759, 2008.
First published February 27, 2008; doi:10.1152/ajpregu.00748.2007.

Impaired lymphatic cerebrospinal fluid absorption in a rat model of kaolin-induced communicating hydrocephalus

G. Nagra,[1] J. Li,[3] J. P. McAllister II,[2] J. Miller,[5] M. Wagshul,[4] and M. Johnston[1]

[1]*Neuroscience Program, Department of Laboratory Medicine and Pathobiology, Sunnybrook Health Sciences Centre, University of Toronto, Toronto, Ontario, Canada;* [2]*Department of Neurosurgery, Division of Pediatric Neurosurgery, University of Utah School of Medicine, Salt Lake City, Utah;* [3]*Department of Neurological Surgery, Wayne State University School of Medicine, University Health Center, Detroit, Michigan;* [4]*Department of Radiology, Stony Brook University, Health Science Center L4-120, Stony Brook, New York; and* [5]*DNA Sequencing and Analysis Facility, Central Michigan University, Mount Pleasant, Michigan*

Submitted 16 October 2007; accepted in final form 27 February 2008

Nagra G, Li J, McAllister JP, II, Miller J, Wagshul M, Johnston M. Impaired lymphatic cerebrospinal fluid absorption in a rat model of kaolin-induced communicating hydrocephalus. *Am J Physiol Regul Integr Comp Physiol* 294: R1752–R1759, 2008. First published February 27, 2008; doi:10.1152/ajpregu.00748.2007.—It has been assumed that the pathogenesis of hydrocephalus includes a cerebrospinal fluid (CSF) absorption deficit. Because a significant portion of CSF absorption occurs into extracranial lymphatics located in the olfactory turbinates, the purpose of this study was to determine whether CSF transport was compromised at this location in a kaolin-induced communicating (extraventricular) hydrocephalus model in rats. Under 1–3% halothane anesthesia, kaolin ($n = 10$) or saline ($n = 9$) was introduced into the basal cisterns of Sprague-Dawley rats, and the development of hydrocephalus was assessed 1 wk later using MRI. After injection of human serum albumin (^{125}I-HSA) into a lateral ventricle, the tracer enrichment in the olfactory turbinates 30 min postinjection provided an estimate of CSF transport through the cribriform plate into nasal lymphatics. Lateral ventricular volumes in the kaolin group (0.073 ± 0.014 ml) were significantly greater than those in the saline-injected animals (0.016 ± 0.001 ml; $P = 0.0014$). The CSF tracer enrichment in the olfactory turbinates (expressed as percent injected/g tissue) in the kaolin rats averaged 0.99 ± 0.39 and was significantly lower than that measured in the saline controls (5.86 ± 0.32; $P < 0.00001$). The largest degree of ventriculomegaly was associated with the lowest levels of lymphatic CSF uptake with lateral ventricular expansion occurring only when almost all of the lymphatic CSF transport capacity had been compromised. We conclude that lymphatic CSF absorption is impaired in a kaolin-communicating hydrocephalus model and that the degree of this impediment may contribute to the severity of the induced disease.

extraventricular hydrocephalus; ventriculomegaly; cribriform plate; olfactory turbinates; arachnoid villi and granulations; lymph; intracranial pressure

HYDROCEPHALUS REPRESENTS A complex and poorly understood family of disorders characterized by expansion of the ventricles within the brain. At a fundamental level, these disorders appear to signify an imbalance between CSF production and absorption. Because overproduction of CSF is relatively rare (27), most investigators have focused on absorption with an implied decrease in CSF transport assumed to contribute significantly to CSF accumulation. Of course, there are many other possible causes of hydrocephalus, and some have argued that ventricular expansion is a secondary consequence of another pathological event, such as the redistribution of CSF pulsations within the cranium (8). Nonetheless, most theories of communicating hydrocephalus incorporate some form of primary or secondary CSF absorption deficit in the pathogenic mechanisms, as it has been demonstrated that CSF outflow resistance is elevated in human hydrocephalus and in animal models designed to simulate this condition (9, 11, 20, 38).

In communicating hydrocephalus, the location of the transport deficit has never been established but, because bulk CSF absorption is believed to occur through the arachnoid villi and granulations, it has always been assumed that the impediment to CSF transport occurs at these structures or somewhere within the extraventricular CSF system (hence, the use of the term extraventricular obstructive hydrocephalus by some investigators) (19). However, the function of the arachnoid projections is increasingly unclear (8, 32, 33, 44).

Although there is some in vitro data using isolated portions of dura that suggest a function for arachnoid projections (40, 41), quantitative experiments in cats, rabbits, monkeys (24–26), and sheep (33, 44) indicate that very little CSF transports into the cranial venous system at normal CSF pressures. The available data suggest that CSF transport can occur into the cranial venous system but only at high intracranial pressures (ICPs) (33, 44). This suggests that a substantial portion of CSF absorption occurs elsewhere, and in this regard, the extracranial lymphatic system has received attention in recent years (reviewed in Ref. 18).

The most important connections between the subarachnoid compartment and extracranial lymphatics appear to exist at the level of the cribriform plate and the olfactory turbinates. The specialized cells of olfaction (olfactory epithelium) are carried on turbinal bodies arising from the ethmoid bone. The turbinates are supported by bone and are covered with a mucous membrane originating at the cribriform plate. The olfactory turbinates contain an extensive lymphatic network, which is in communication with the subarachnoid space through specialized connections with the olfactory nerves (16, 42–44). Once CSF enters the initial lymphatics, it is then transported via

Address for reprint requests and other correspondence: M. G. Johnston, Neuroscience Research, Sunnybrook Health Sciences Centre, Univ. of Toronto, Research Bldg., S-111, 2075 Bayview Ave., Toronto, Ontario, M4N 3M5 (e-mail: miles.johnston@sunnybrook.ca) or J. P. (Pat) McAllister, Division of Pediatric Neurosurgery, University of Utah School of Medicine, 175 N. Medical Drive East, Salt Lake City, UT 84132-2303 (e-mail: pat.mcallister@hsc.utah.edu).

The costs of publication of this article were defrayed in part by the payment of page charges. The article must therefore be hereby marked "*advertisement*" in accordance with 18 U.S.C. Section 1734 solely to indicate this fact.

cervical lymphatic ducts to the venous system at the base of the neck. There is abundant quantitative and qualitative evidence to suggest that extracranial lymphatic vessels have an important role in CSF absorption (1–4, 29, 32). These pathways also seem to be relevant in humans and nonhuman primates (12, 13).

As a natural progression to these studies, it seemed relevant to consider whether some disorders of the CSF system (most notably hydrocephalus) might be related to a disruption in lymphatic CSF transport. In the experiments reported here, we used a rat kaolin-induced communicating hydrocephalus model to test the hypothesis that ventriculomegaly may be related to impaired lymphatic function. Kaolin injections have been used extensively to produce obstructive hydrocephalus in a variety of neonatal, juvenile, and adult animal models (7, 15, 21). In many applications, kaolin administration is used to block the outlets of the fourth ventricle leading to obstructive or noncommunicating hydrocephalus. These approaches have yielded valuable data on the pathophysiology that appears secondary to ventriculomegaly. In contrast, as described in detail elsewhere (19), the injection of kaolin into the basal cisterns (the method employed in this report) does not obstruct the fourth ventricular outlets and produces a communicating, or extraventricular form, of hydrocephalus.

The main objective of the studies reported here was to test whether CSF uptake into ethmoidal lymphatic vessels was compromised in a kaolin-induced communicating hydrocephalus model in rats. We observed that in cases of severe ventricular dilation, there was a marked reduction in CSF access to lymphatic vessels at the level of the cribriform plate.

MATERIALS AND METHODS

A total of 54 female Sprague-Dawley rats with an average weight of 246.01 ± 2.41 g were used for this investigation (purchased from Harlan, Indianapolis, IN and Harlan, Montreal, Quebec, Canada). The animals were fed lab rat chow (LabDiet 5001) until death.

The injections of kaolin or saline were performed in the laboratory of Dr. McAllister at the Wayne State University School of Medicine according to the protocol approved by the institutional Animal Investigation Committee. The lymphatic studies were carried out in Dr. Johnston's laboratory at Sunnybrook Health Science Centre in Toronto. These experiments were approved by the ethics committee at the Sunnybrook Health Science Centre and conformed to the guidelines set by the Canadian Council on Animal Care and the Animals for Research Act of Ontario.

MRI studies (to determine ventricle sizes) were performed about 1 wk after the injection of saline (average 8.7 ± 1.5 days) or kaolin (average 7.8 ± 0.1 days) into the basal cisterns. The animals were then sent to Toronto for lymphatic analysis about 1 wk after this (average time from induction of hydrocephalus to lymphatic studies were 17.3 ± 1.2 days for saline- and 15.0 ± 0.6 days for kaolin-injected rats).

Induction of communicating hydrocephalus. As described in detail previously (19), the rats were anesthetized with a mixture of 1–3% halothane with 40% oxygen, and using aseptic techniques, we incised the skin along the ventral midline of the neck. After the soft tissues were reflected to expose the base of the skull, a 30-gauge needle, custom bent to 30°, was inserted into the subarachnoid space between the clivus and the C1 vertebra. The needle was advanced 1.5–2.0 mm along the inner surface of the cranial cavity, and a 50-μl sterile suspension of 25% kaolin in saline was injected at the rate of about 6 μl/s. The surgical incision was closed in layers using absorbable suture (Vicryl), and the rats were allowed to recover. Postoperatively, butorphenol was given subcutaneously (0.05–2.0 mg/kg) every 4–8 h as needed to control pain. Animals that experienced breathing difficulty (coughing) or symptoms of life-threatening increases in intracranial pressure (ICP) postoperatively received mannitol (1.5 g/kg iv). Sham controls were prepared in a similar fashion but received sterile saline only (308 mOsM/l, pH 7.4).

Assessment of ventricular size. MRI was used at Wayne State University to measure ventricular size in vivo. After anesthesia with a mixture of 87 mg/kg ketamine plus 13 mg/kg xylazine, the animal was placed into a 4.7-T magnet, and coronal and sagittal T1- and T2-weighted images were obtained (TE/TR = 20/700 ms and 67/5000 ms, respectively) on 1.0-mm slice thickness. Ventricular volumes (lateral and 3rd ventricles) were calculated from T2 images, starting from the center of the cerebral aqueduct up to the anterior-most portion of the lateral ventricles. The volumetric calculations were semiautomated as follows; an appropriate intensity threshold was first chosen to exclude background tissue and to highlight the bright ventricles. This was followed by careful inspection of each image, and manual tracing was used to correct any areas of the ventricle, which had been incorrectly deleted, or to delete nonventricular regions that had been incorrectly included. This process resulted in a binary mask of ventricular pixels, which when multiplied by the volume of each pixel and summed over all slices produced the net ventricular volume in milliliters. The Evan's ratio was taken at the level of the Foramen of Monroe as the maximum width of both lateral ventricles divided by the maximum width of the brain at this level.

Assessment of lymphatic CSF absorption. The development of the method to assess lymphatic CSF uptake in the rat has been described in a previous publication (31). The rapid movement of CSF tracers (dyes or radioactive proteins) into the olfactory turbinates supports a role for lymphatics in CSF absorption and provides the basis of the method used in this report to assess the impact of hydrocephalus on lymphatic CSF transport.

Rats were anesthetized initially by placement in a custom-built rodent anesthesia chamber using halothane (4–5%) in oxygen. For the experimental procedure, they were maintained with 2–2.5% halothane in oxygen delivered by a nose cone (rat anesthesia mask, model 906, Kopf Instruments,Tujunga, CA). The animals were placed on a heating pad (Fine Science Tools, Vancouver, BC, Canada) and fixed in position in a Small Animal Stereotaxic device (Kopf Instruments, model 900). The skin over the cranium was removed, and the junction of the sagittal and coronal sutures was identified. A small high-speed microdrill with a rounded tip (Fine Science Tools, Vancouver, BC, Canada) was used to grind away the bone to expose the dural membrane.

A 50-μl Hamilton syringe (Fisher Scientific, Toronto, Ontario, Canada) with a 30-gauge needle was used at 0.92 mm posterior and 1.4 mm lateral to the bregma, and 3.3 mm deep to the dural membrane at the left or right hemisphere. The coordinates were noted from the stereotaxic instrument and adjusted according to the reference values from a rat brain atlas (34). The needle was loaded with ^{125}I-labeled human serum albumin (HSA), and the tip was lowered into a lateral ventricle (because ventriculomegaly developed bilaterally in all cases, either the right or left ventricles was used randomly). Fifty microliters containing 500 μg of ^{125}I-labeled HSA (0.93 MBq/ml, 10 mg/ml, DraxImage, Kirkland, Quebec, Canada) was injected over 30 s into a lateral ventricle. The needle was removed after 1–2 min, and the needle path was sealed with bone wax. After variable periods, the animals were killed by injection of 1.0 ml euthanyl (ip). Immediately before death, a blood sample was taken from the heart. After death, the kidney and the spleen were removed, and samples from liver, skeletal muscle, and tail were collected. All tissue samples were placed into preweighed glass test tubes for weight determination using a Mettler BB2400 balance. The carcasses were then frozen for at least 24 h in a freezer.

To facilitate the assessment of radioactivity in the olfactory submucosa and to prevent potential postmortem tracer contamination

from the CSF compartment, a portion of the turbinates was cut from frozen tissue. The upper, lower, and middle olfactory turbinates were excised with a fine-tooth saw, as described in detail in our previous paper and assessed separately for radioactivity (31). The upper portion represented partial superior cells of the ethmoid turbinates along with cartilage and soft tissues of the nasal wall. The middle portion contained the main portion of the turbinates (henceforth termed the middle turbinates). The lower portion consisted of a fraction of the posterior cells of the turbinates and part of the hard palate. The samples were weighed as described above and were monitored for radioactivity in a multichannel gamma spectrometer (Compugamma, LKB Wallac, Turku, Finland).

Evan's blue dye (2%) was used to visualize the movement of CSF across the cribriform plate postmortem in two kaolin- and two saline-injected rats. The animals were anesthetized as described above. Following a midline incision, the skin was reflected over the cranium. An Alzet rat brain cannula (Direct Corporation, Cupertino, CA) was inserted into the cortex with the tip positioned in the lateral ventricle. The cannula was secured to the skull with Surehold glue (mixture of ethyl cyanoacrylate and polymethylmethacrylate; Surehold, Chicago, IL). Immediately after death, 0.3 ml of Evan's blue dye was infused over 30 s into the lateral ventricle. The animals were frozen overnight and after decapitation, the heads were sectioned in preparation for photographic studies. The images were captured on a Nikon digital camera (Coolpix 995, Henry's Camera, Toronto, ON, Canada).

Analysis of data. In the first group of experiments, we determined the most appropriate time after injection of the radioactive tracer to assess the tracer enrichment in the olfactory turbinates (30 animals total with 6 rats at each time of 10, 20, 30, 40, and 60 min). In a second group, we used Evans blue dye in an attempt to visualize CSF-lymphatic connections in two saline- and two kaolin-injected rats. In the final group, we examined the lymphatic uptake of the tracer in 10 saline- or 10 kaolin-injected animals (1 animal in the saline group died during the experiment and could not be used in the data analysis). The enrichment of the CSF tracer in various tissues was expressed as a percent injected dose per gram of tissue. All data were expressed as the means ± SE. The data were analyzed with an unpaired two-sample *t*-test and a Wilcoxon nonparametric equivalent. We interpreted $P < 0.05$ as significant.

RESULTS

Development of hydrocephalus. Most rats undergoing kaolin injections exhibited relatively normal behavior postoperatively, although many of the kaolin-injected animals exhibited bloody nasal and orbital secretions and coughed frequently. We presumed that these symptoms related to increases in ICP, although no pressures were measured in this study. The coughing either disappeared normally within a few days or was alleviated by administration of mannitol, which is known to reduce CSF pressure. Regardless of how severe ventriculomegaly had become, no animals exhibited signs of cranial enlargement.

MRI analysis revealed that nearly all kaolin deposits on the ventral brain stem were bilateral and contiguous. The largest formations extended from the medulla to the interpeduncular fossa, and all covered a portion of the pons. Some kaolin deposits were small and located unilaterally. No kaolin deposits blocked the foramina of Luschka grossly or occupied the cisterna magna. Most importantly, no kaolin deposits were located anterior to the optic chiasm, including the region of the cribriform plate.

Compared with saline-injected controls, the ventricular system expanded to relatively moderate and severe levels in most kaolin-injected animals (examples in Fig. 1, *A* and *B*). All portions of the ventricular system exhibited expansion. Enlargement of the lateral ventricles was symmetrical and proportionally greater than other regions of the ventricular system. The cerebral aqueduct was patent and dramatically expanded posteriorly. This indicated that the hydrocephalus in this model is of the communicating type. More details on the morphological changes that accompany this model have been described previously (19).

Figure 1 also illustrates the average ventricular volumes (*C*) and Evans ratios (*D*) in the two groups. In the kaolin-injected rats, the ventricular volumes were significantly greater (ranging from 0.015 to 0.162 ml, average 0.073 ± 0.014 ml) than those observed in the saline-injected animals (ranging from 0.011 to 0.022 ml, average 0.016 ± 0.001 ml). In the kaolin-injected group, the Evans ratios ranged from 0.36 to 0.58 (average 0.48 ± 0.02) and were significantly greater than those in the saline-injected animals (ranging from 0.25 to 0.39, average 0.35 ± 0.01).

Assessment of CSF transport through cribriform plate. Before the hydrocephalus experiments, we conducted a study to determine the most appropriate time to assess tracer enrichment in the olfactory turbinates of Sprague-Dawley rats. The data are illustrated in Fig. 2. The highest concentrations of ^{125}I-HSA were found consistently in the middle turbinate area (average weights 0.36 ± 0.03 g), which represented the bulk of the olfactory turbinates. For this reason, we chose to assess the lymphatic uptake of CSF using tracer enrichment in the middle turbinates. The lower turbinates also contained high concentrations of the tracer. The tracer enrichment at these locations was much greater than that observed in blood (up to 40 min). The radioactivity in the top turbinates was similar to that observed in blood. Tracer recoveries in skeletal muscle, spleen, kidney, liver, and tail were much lower than those observed in the lower and middle turbinates and likely were reflective of the tracer within the vasculature of these tissues (not illustrated in Fig. 2). On average, tracer concentrations in the middle and bottom turbinates peaked at 30 min after ventricular injection. This time was chosen to compare the transport of the CSF tracer across the cribriform plate in the kaolin- and saline-injected animals.

Transport of CSF tracer into olfactory turbinates: comparison between kaolin- and saline-injected animals. Initial studies were performed with Evan's blue dye injected into the lateral ventricles to visualize the movement of the contrast agent within the CSF system and its possible entry into the olfactory turbinates. Evan's blue dye was observed in the lateral ventricles and subarachnoid space of both kaolin- and saline-injected animals. However, the appearance of dye in the olfactory turbinates was much less prominent in the kaolin-injected animals compared with the saline-injected group. Examples of the appearance of Evan's blue dye in the saline- and kaolin-injected animals are provided in Fig. 3*A* and *B*, respectively.

Figure 3*C* illustrates two examples of tracer enrichment in one saline-injected (ventricular volume − 0.020 ml) and one kaolin-injected animal (ventricular volume − 0.099 ml). The ^{125}I-HSA enrichment in the olfactory turbinates was much less in the kaolin-injected animal. Although it would appear that tracer enrichment in the other tissues was also less in this kaolin-injected rat, this was not a consistent pattern for all animals.

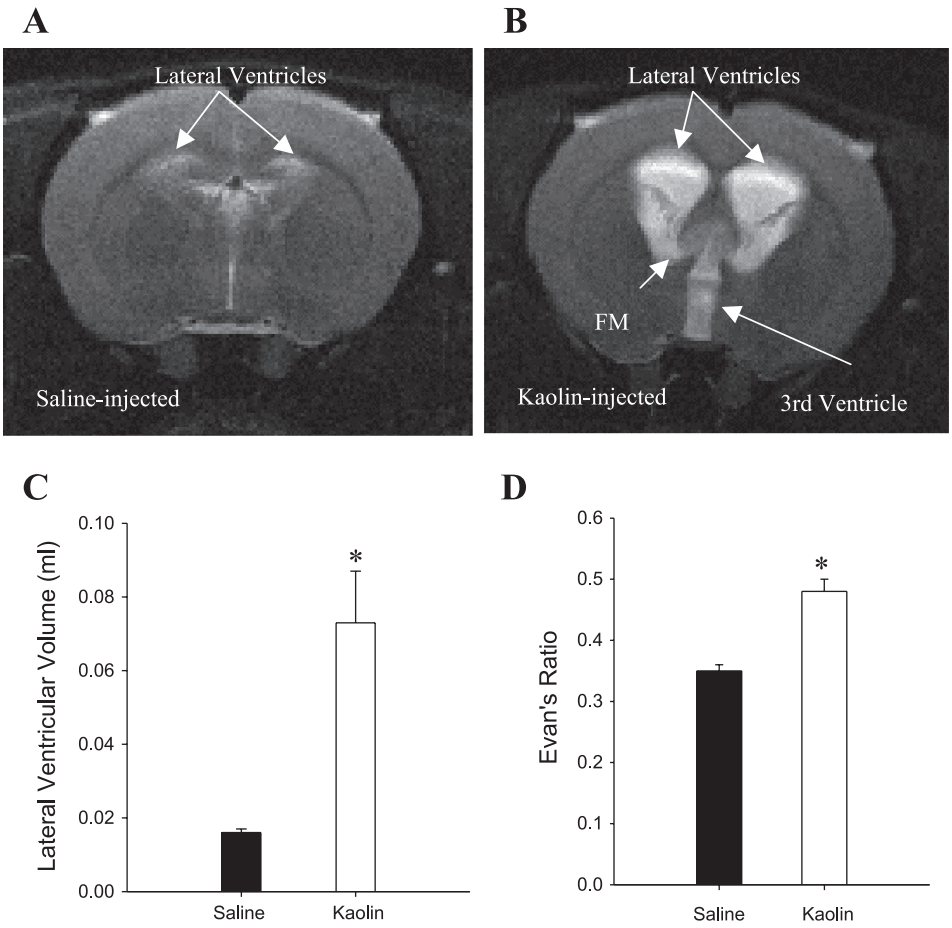

Fig. 1. Impact of saline or kaolin injection on the ventricular volumes and Evans ratios. Representative MRI images of saline- (*A*) and kaolin- (*B*) injected animals to illustrate the extent of ventriculomegaly achieved in the latter group. These coronal sections taken ~1 wk after injection show the bilateral enlargement of the frontal horns of the lateral ventricles at the foramina of Monro (FM), as well as the expansion of the third ventricle in the kaolin-injected animal. Ventricular volumes (*C*) and Evans ratios (*D*) are also illustrated. A two-sample unpaired *t*-test ($P = 0.0014$) and a two-sided Wilcoxon nonparametric test ($P = 0.0042$) indicated that the ventricular volumes for the kaolin group ($n = 10$) were significantly higher than those measured in the saline-injected animals ($n = 9$). Similar analysis of the Evans ratios revealed significant differences in the saline and kaolin-injected rats [two-sample unpaired *t*-test, $*P = 0.0001$; Two-sided Wilcoxon nonparametric test ($P = 0.0042$)].

Figure 4*A* illustrates the average middle turbinate enrichment data assessed at 30 min after tracer injection. The movement of the CSF tracer across the cribriform plate in the kaolin-injected rats was significantly less than that measured in the saline group. Indeed, the tracer enrichment in the kaolin animals was only 17% of that observed in the controls. Although the tracer concentration in blood appears to be higher in the kaolin group (Fig. 4*A, inset*), these differences were not significant. Additionally, there were no saline/kaolin-related significant differences in the radioactivity measured in any of the other tissues (data not illustrated).

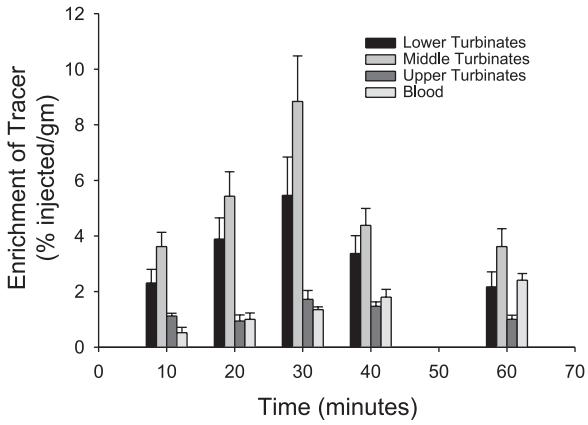

Fig. 2. Average cerebrospinal fluid (CSF) tracer enrichment (percent injected dose/g tissue) in the olfactory turbinates and blood as a function of time ($n = 6$ at each time). Tracer enrichment in the lower and middle olfactory turbinates was greater than that measured in the upper turbinates or blood and peaked at 30 min after tracer injection into a lateral ventricle. Tracer concentrations in skeletal muscle, spleen, kidney, liver, and tail were very low and are not illustrated in the figure.

Figure 4*B* illustrates the ventricular volumes for all saline- ($n = 9$, solid circles) and kaolin-injected animals ($n = 10$, open circles) plotted against the corresponding 30-min middle turbinate enrichment data for these rats. The exponential-like relationship suggests that the largest ventricles (most severe hydrocephalus) were associated with the lowest CSF transport into ethmoidal lymphatic vessels. Indeed, ventricular volumes did not appear to increase until almost all of the tracer movement across the cribriform plate had been abolished.

DISCUSSION

Our major objective was to assess lymphatic CSF absorption in a kaolin-induced rat model of communicating hydrocephalus using a radioactive protein tracer. The clearance of albumin from the subarachnoid space is proportional to bulk flow (36), and various tracer methods have been used to estimate lymphatic CSF transport as outlined in our previous studies (2). In the method reported here, the tracer (introduced into a lateral ventricle) travels rapidly to the subarachnoid space surrounding the olfactory bulbs and passes through the cribriform plate to reach the lymphatic vessels located in the olfactory turbinates. By sampling the turbinate tissues, we were able to

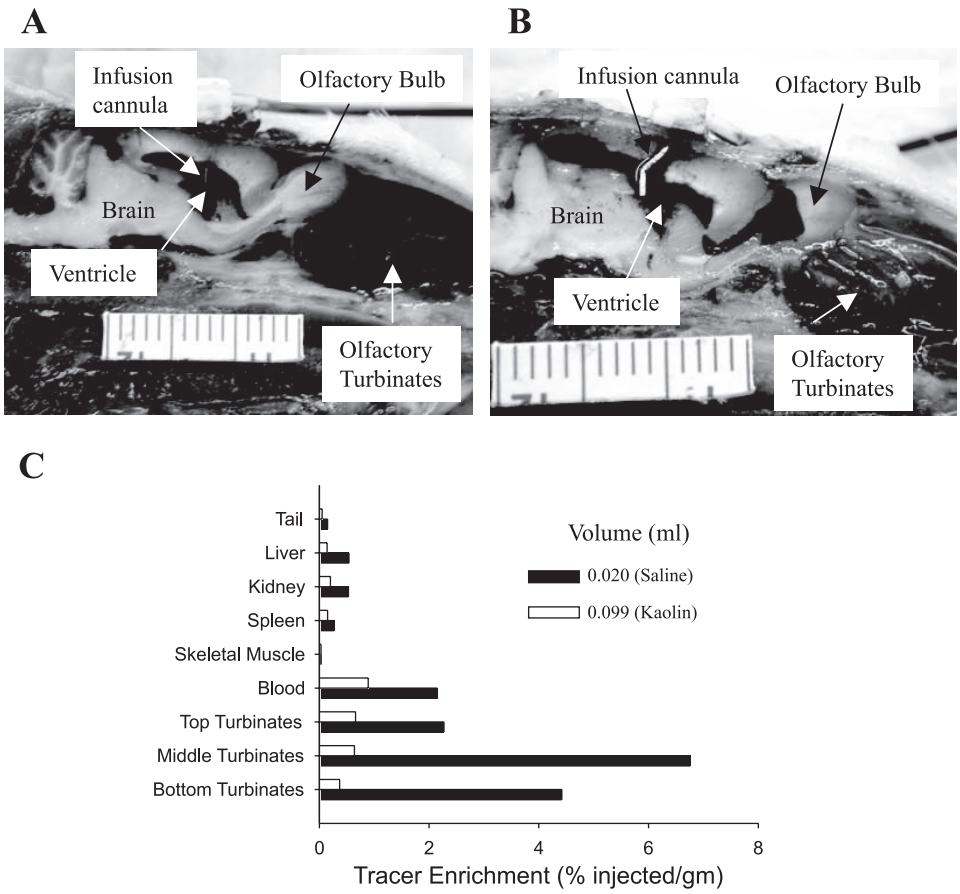

Fig. 3. Comparison of lymphatic CSF absorption in the saline- and kaolin-injected animals. Sagittal section of a saline- (*A*) and kaolin- (*B*) injected animal. Evan's blue dye was injected into a lateral ventricle post mortem. The turbinates of the saline-injected animal are densely stained with the dye. In contrast, the turbinates of the kaolin-injected animal contained less dye. The scale in millimeters is provided at the bottom of the images. *C*) Examples of the distribution of radioactivity into various tissues after ^{125}I-HSA injection into a lateral ventricle. Solid bars represent data from a saline-injected rat. Open bars illustrate data from a kaolin-injected animal. The ventricular volumes for both examples are provided in the inset. The enrichment of the tracer in the turbinate tissues in the saline example was much greater than that in the kaolin-injected rat. In the latter case, the ventricles were enlarged (0.099 ml compared with 0.020 ml for the saline animal).

obtain a quantitative estimate of lymphatic absorption at this location (31).

The data in this report indicate that the transport of a CSF protein across the cribriform plate was reduced significantly in this hydrocephalus model. On the basis of assessments with MRI, the injection of kaolin into the basal cisterns induced a communicating form of hydrocephalus in the majority of animals. This model appears to replicate neonatal or infantile forms of hydrocephalus in that ventriculomegaly developed within days of induction and moderate to severe levels of enlargement were observed in most animals. Kaolin administration in adult animals with fixed skulls does not normally produce rapid or severe ventricular expansion; rather, such progression is usually found only in young animals with expandable skulls (10, 22, 23).

Further evidence suggesting some relationship between hydrocephalus and lymphatic function comes from mouse experiments in which intrathecal injections of TGF-β1 were used to induce hydrocephalus. In these studies, ink was administered into the lateral ventricles and the time taken for the ink to stain the cervical lymph nodes was lengthened considerably compared with the nonhydocephalic animals (28, 39). This suggested that the cribriform-lymphatic connection is also disrupted in the TGFβ_1-induced hydrocephalus model.

The relationship between a CSF absorption deficit and ventricular expansion is no doubt, a very complex issue. Figure 4*B* demonstrates an unusual nonlinear relationship between lymphatic function and ventricular volume. It would seem that bulk flow could be perturbed significantly before there was any evidence of ventricular expansion. Indeed, from the graph, it would appear that almost all of the lymphatic bulk flow capacity must be compromised before significant hydrocephalus develops. This implies that the CSF absorption system has significant excess capacity and that pathology does not develop until this capacity is largely consumed. Perhaps there is a critical breakpoint in the bulk flow-ventricular volume relationship that has not been appreciated in the past.

It seems likely that the host can afford to lose a certain (unknown) number of CSF absorption sites, as presumably, other locations or mechanisms can compensate up to a certain extent. The absorption of CSF from the spinal subarachnoid compartment would be a good example (5). In support of this, we noted previously that CSF outflow resistance increased when CSF transport through the cribriform plate was obstructed (37), but this increase was much more evident when CSF absorption from the spinal cord was prevented (29, 32). As more and more CSF absorption sites become blocked, the diminished CSF absorptive capacity would be reflected by reduced CSF (and thus tracer) clearance to plasma. As can be observed in Fig. 4*A* (*inset*), the average blood levels of the tracer were slightly higher than in the saline group, although not significantly so. This suggests that other pathways might have compensated for the diminished absorption at the cribriform plate.

One possibility in this regard is the arachnoid villi and granulations. Although a role for these elements in CSF absorption under normal conditions is increasingly being challenged, there is evidence to suggest that CSF may be trans-

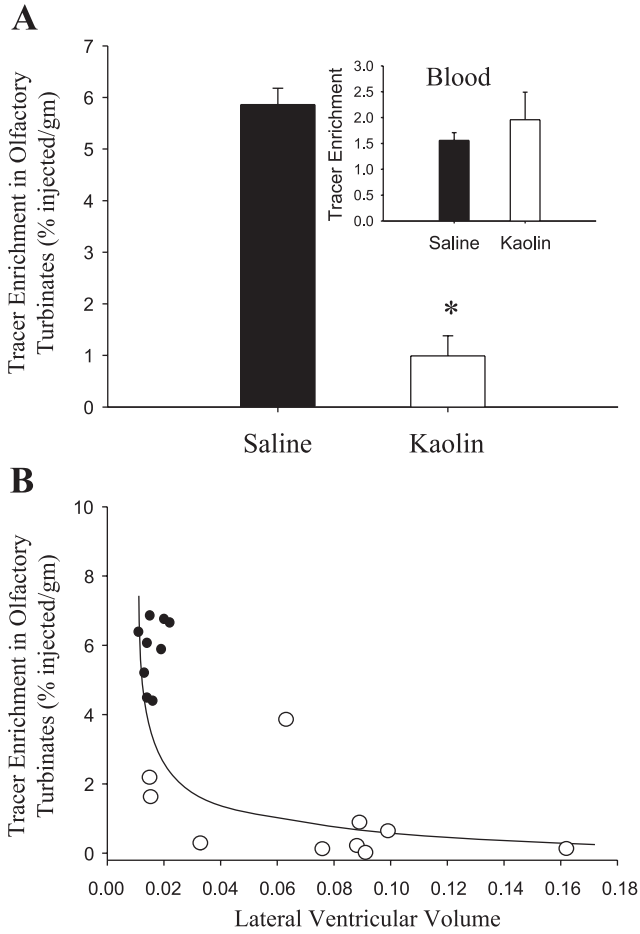

Fig. 4. Comparison of lymphatic CSF absorption in the saline ($n = 9$) and kaolin-injected animals ($n = 10$). One saline-injected rat died before tracer assessment. *A*: Impact of saline or kaolin injection on the middle turbinate enrichment of the CSF tracer. The movement of the CSF tracer across the cribriform plate in the kaolin-injected rats was significantly less that that measured in the saline group (two-sample unpaired *t*-test, $*P < 0.0001$; two-sided Wilcoxon nonparametric test, $*P < 0.0001$). The tracer concentrations in the blood in the two groups are illustrated in the inset to *A* (no significant differences). *B*: A plot of the turbinate enrichment of tracer vs. ventricle size yielded an exponential relationship (saline-injected, ●; kaolin-injected, ○). These data suggested that the largest ventricles (most severe hydrocephalus) were associated with the lowest CSF transport into ethmoidal lymphatic vessels.

ported from the subarachnoid space into the cranial veins at high ICPs (33, 44). Therefore, the recruitment of additional absorption sites at the level of the arachnoid granulations and villi might temper the impact of the loss of lymphatic CSF absorption.

It is, of course, theoretically possible that the function of the arachnoid projections was also diminished after kaolin administration, but we do not believe that this was the case. In this regard, it is interesting to compare the impact of kaolin injection into the basal cisterns with the effects of kaolin administration over the cerebral convexities (19). In both cases, the ventricles expanded, but the ventriculomegaly associated with convexity injections was less severe and much more protracted, requiring 3 or 4 mo to develop compared with the ventriculomegaly produced by basal cistern injections, which developed quickly. With this in mind, we think it unlikely that CSF absorption through the arachnoid projections was compromised when kaolin was administered into the basal cisterns ~2 wk before assessment of lymphatic function.

The lymphatic absorption deficit could be due to restricted access of CSF to absorption sites at the base of the brain, some blockage in the foramina of the cribriform plate, or the impact of kaolin directly on the lymphatic vessels themselves.

It is possible that kaolin particles were dislodged from the original injection site and migrated to other areas to form multiple foci of obstruction (fibrosis) or inflammation. Certainly, collagen deposits have been observed in other rat models of hydrocephalus. When fibroblast growth factor-2 is introduced into the ventricular system of rats, an *ex vacuuo* type of hydrocephalus develops, which is characterized by elevations in CSF pressure and CSF outflow resistance (11). These changes were attributed, in part, to fibrosis in the arachnoid membrane. Along these lines, a kaolin-induced inflammatory response might generate proinflammatory substances that elicit fibrosis in the subarachnoid space or in the cribriform plate foramina. If this were the case, CSF movement into extracranial lymphatics might be compromised. However, kaolin deposits in the area of the olfactory bulb and cribriform plate were never observed in gross postmortem examinations of the animals used in this study, and thus we do not believe that kaolin had a direct effect on the foramina of the cribriform plate or on the nasal lymphatics themselves.

Venous hypertension has been postulated as a contributing factor in hydrocephalus development (35). It has been assumed that an increase in intracranial venous pressure would alter the CSF-venous pressure gradient and thus compromise CSF absorption through the arachnoid granulations and villi (14). Assuming that the venous hypertension in the cranium would be reflected to the veins in the base of the neck, this phenomenon could also theoretically reduce lymphatic CSF transport since lymph flow would have to overcome the elevated outflow pressures expressed in the venous system. However, water is removed from lymph as it transits from the base of the brain to the veins located at the base of the neck (17). This tends to "depressurize" the lymphatic system and reduce the impact of elevated inflow to the vessels or increased outflow resistance. Therefore, although we do not know whether venous pressures are elevated in the kaolin model, we think it unlikely that venous hypertension will have any long-term impact on the transport of CSF into the lymphatics associated with the olfactory turbinates.

From a lymphatic perspective, we can obtain some idea of the impact of reduced CSF transport through the cribriform plate from studies in which the plate has been sealed on the extracranial surface. These reports indicate that experimental obstruction of the cribriform plate reduces cranial CSF absorption (29, 32), elevates cranial CSF outflow resistance (37), and increases ICP (30).

One might expect that ICP would rise with any obstruction to CSF outflow. However, it is not apparent how disruption of CSF transport through the cribriform plate would lead to a transmantle pressure gradient favoring enlargement of the ventricles since CSF pressure would likely rise equally in all CSF spaces within the cranium. One possibility is that impaired lymphatic CSF uptake could affect compliance and cause a redistribution of pulsatility within the cranium. One group has postulated that this could lead to ventriculomegaly (8), but this concept will need to be tested in future experi-

ments looking at changes in pulsatility in the kaolin model. In any event, the data in this report suggest an association between ventricular size and lymphatic function. Whether this perceived interaction originates from a direct cause-and-effect relationship or rather, arises secondarily from a complex interplay of other unknown physiological parameters, requires further investigation.

Perspectives and Significance

We believe that the data outlined in this report represent the first demonstration of a CSF absorption deficit at a discrete anatomical location. This may be especially significant since the site in question is not part of the conventional view of CSF absorption. The notion that CSF is formed largely in the choroid plexus and is absorbed primarily through arachnoid villi and granulations provides the cornerstone of our understanding of hydrocephalus. This viewpoint has existed for many years, but unfortunately, it has not provided fertile ground for the development of new therapeutic approaches to hydrocephalus beyond the physical diversion of CSF with shunts or the endoscopic third ventriculostomy procedure. Hydrocephalus continues to be an important neurosurgical problem and shunt obstruction due to various causes remains an important clinical issue (6). Attention directed to the cribriform plate and the lymphatic vessels within the olfactory turbinates may reveal new insights into the cause of hydrocephalus and could ultimately lead to the development of novel targets for therapeutic intervention.

ACKNOWLEDGMENTS

We wish to thank M. Katic (Department of Research Design and Biostatistics, Sunnybrook Health Sciences Centre) for assistance in the computational analyses of the data.

GRANTS

This research was funded by the Canadian Institutes of Health Research Grant (7925) and the Brain Child Foundation (USA).

REFERENCES

1. **Boulton M, Flessner M, Armstrong D, Hay J, Johnston M.** Lymphatic drainage of the CNS: effects of lymphatic diversion/ligation on CSF protein transport to plasma. *Am J Physiol Regul Integr Comp Physiol* 272: R1613–R1619, 1997.
2. **Boulton M, Flessner M, Armstrong D, Hay J, Johnston M.** Determination of volumetric cerebrospinal fluid absorption into extracranial lymphatics in sheep. *Am J Physiol Regul Integr Comp Physiol* 274: R88–R96, 1998.
3. **Boulton M, Flessner M, Armstrong D, Mohamed R, Hay J, Johnston M.** Contribution of extracranial lymphatics and arachnoid villi to the clearance of a CSF tracer in the rat. *Am J Physiol Regul Integr Comp Physiol* 276: R818–R823, 1999.
4. **Boulton M, Young A, Hay J, Armstrong D, Flessner M, Schwartz M, Johnston M.** Drainage of CSF through lymphatic pathways and arachnoid villi in sheep: measurement of 125I-albumin clearance. *Neuropathol Appl Neurobiol* 22: 325–333, 1996.
5. **Bozanovic-Sosic R, Mollanji R, Johnston MG.** Spinal and cranial contributions to total cerebrospinal fluid transport. *Am J Physiol Regul Integr Comp Physiol* 281: R909–R916, 2001.
6. **Del Bigio MR.** Biological reactions to cerebrospinal fluid shunt devices: a review of the cellular pathology. *Neurosurgery* 42: 319–325, 1998.
7. **Del Bigio MR, Wilson MJ, Enno T.** Chronic hydrocephalus in rats and humans: white matter loss and behavior changes. *Ann Neurol* 53: 337–346, 2003.
8. **Egnor M, Zheng L, Rosiello A, Gutman F, Davis R.** A model of pulsations in communicating hydrocephalus. *Pediatr Neurosurg* 36: 281–303, 2002.
9. **Gjerris F, Borgesen SE, Schmidt J, Sorensen PS.** Resistance to cerebrospinal fluid outflow in patients with normal pressure hydrocephalus. In: *Outflow of Cerebrospinal Fluid*, edited by Gjerris F, Borgesen SE, and Sorensen PS. Copenhagen: Munksgaard, 1989.
10. **Hale PM, McAllister JP, Katz SD, Wright LC, Lovely TJ, Miller DW, Wolfson BJ, Salotto AG, Shroff DV.** Improvement of cortical morphology in infantile hydrocephalic animals after ventriculoperitoneal shunt placement. *Neurosurgery* 31: 1085–1096, 1992.
11. **Johanson CE, Szmydynger-Chodobska J, Chodobski A, Baird A, McMillan P, Stopa EG.** Altered formation and bulk absorption of cerebrospinal fluid in FGF-2-induced hydrocephalus. *Am J Physiol Regul Integr Comp Physiol* 277: R263–R271, 1999.
12. **Johnston M, Zakharov A, Koh L, Armstrong D.** Subarachnoid injection of Microfil reveals connections between cerebrospinal fluid and nasal lymphatics in the non-human primate. *Neuropathol Appl Neurobiol* 31: 632–640, 2005.
13. **Johnston M, Zakharov A, Papaiconomou C, Salmasi G, Armstrong D.** Evidence of connections between cerebrospinal fluid and nasal lymphatic vessels in humans, non-human primates and other mammalian species. *Cerebrospinal Fluid Res* 1: 2, 2004.
14. **Jones HC, Gratton JA.** The effect of cerebrospinal fluid pressure on dural venous pressure in young rats. *J Neurosurg* 71: 119–123, 1989.
15. **Khan OH, Enno TL, and Del Bigio MR.** Brain damage in neonatal rats following kaolin induction of hydrocephalus. *Exp Neurol* 200: 311–320, 2006.
16. **Kida S, Pantazis A, Weller RO.** CSF drains directly from the subarachnoid space into nasal lymphatics in the rat. Anatomy, histology and immunological significance. *Neuropathol Appl Neurobiol* 19: 480–488, 1993.
17. **Koh L, Nagra G, Johnston M.** Properties of the lymphatic cerebrospinal fluid transport system in the rat: impact of elevated intracranial pressure. *J Vasc Res* 44: 423–432, 2007.
18. **Koh L, Zakharov A, Johnston M.** Integration of the subarachnoid space and lymphatics: is it time to embrace a new concept of cerebrospinal fluid absorption? *Cerebrospinal Fluid Res* 2: 6, 2005.
19. **Li J, McAllister II JP, Wagshul ME, Miller JM, Johnston MG, Haacke M, Walker ML.** Communicating hydrocephalus in adult rats with obstruction of the basal cisterns or the cortical subarachnoid space. *Exp Neurol* (January 31, 2008). doi:10.1016/j.expneurol.2007.12.030.
20. **Malm J, Lundkvist B, Eklund A, Koskinen LO, Kristensen B.** CSF outflow resistance as predictor of shunt function. A long-term study. *Acta Neurol Scand* 110: 154–160, 2004.
21. **McAllister JP, Chovan P.** Neonatal hydrocephalus. Mechanisms and consequences. *Neurosurg Clin N Am* 9: 73–93, 1998.
22. **McAllister JP, Cohen MI, O'Mara KA, Johnson MH.** Progression of experimental infantile hydrocephalus and effects of ventriculoperitoneal shunts: an analysis correlating magnetic resonance imaging with gross morphology. *Neurosurgery* 29: 329–340, 1991.
23. **McAllister JP, Maugans TA, Shah MV, Truex RC Jr.** Neuronal effects of experimentally induced hydrocephalus in newborn rats. *J Neurosurg* 63: 776–783, 1985.
24. **McComb JG, Hyman S.** Lymphatic drainage of cerebrospinal fluid in the cat. In: *Hydrocephalus*, edited by Shapiro, K., Marmarou, A., and Portnoy, H. New York: Raven, 1984.
25. **McComb JG, Davson H, Hyman S, Weiss MH.** Cerebrospinal fluid drainage as influenced by ventricular pressure in the rabbit. *J Neurosurg* 56: 790–797, 1982.
26. **McComb JG, Hyman S.** Lymphatic drainage of cerebrospinal fluid in the primate. In: *Pathophysiology of the Blood-Brain Barrier*, edited by Johansson BB and Widner H. New York: Elsevier Science Publishers, 1990.
27. **Milhorat TH.** *Neurosurgery.* New York: McGraw Hill, 1985, p. 2135–2139.
28. **Moinuddin SM, Tada T.** Study of cerebrospinal fluid flow dynamics in TGF-beta 1 induced chronic hydrocephalic mice. *Neurol Res* 22: 215–222, 2000.
29. **Mollanji R, Bozanovic-Sosic R, Silver I, Li B, Kim C, Midha R, Johnston M.** Intracranial pressure accommodation is impaired by blocking pathways leading to extracranial lymphatics. *Am J Physiol Regul Integr Comp Physiol* 280: R1573–R1581, 2001.
30. **Mollanji R, Bozanovic-Sosic R, Zakharov A, Makarian L, Johnston MG.** Blocking cerebrospinal fluid absorption through the cribriform plate increases resting intracranial pressure. *Am J Physiol Regul Integr Comp Physiol* 282: R1593–R1599, 2002.
31. **Nagra G, Koh L, Zakharov A, Armstrong D, Johnston M.** Quantification of cerebrospinal fluid transport across the cribriform plate into

lymphatics in rats. *Am J Physiol Regul Integr Comp Physiol* 291: R1383–R1389, 2006.
32. **Papaiconomou C, Bozanovic-Sosic R, Zakharov A, Johnston M.** Does neonatal cerebrospinal fluid absorption occur via arachnoid projections or extracranial lymphatics? *Am J Physiol Regul Integr Comp Physiol* 283: R869–R876, 2002.
33. **Papaiconomou C, Zakharov A, Azizi N, Djenic J, Johnston M.** Reassessment of the pathways responsible for cerebrospinal fluid absorption in the neonate. *Childs Nerv Syst* 20: 29–36, 2004.
34. **Paxinos G, Watson C.** *The Rat Brain in Stereotaxic Coordinates*. San Diego: Academic Press, 1997.
35. **Portnoy HD, Branch C, Castro ME.** The relationship of intracranial venous pressure to hydrocephalus. *Childs Nerv Syst* 10: 29–35, 1994.
36. **Rudick RA, Zirretta DK, Herndon RM.** Clearance of albumin from mouse subarachnoid space: a measure of CSF bulk flow. *J Neurosci Methods* 6: 253–259, 1982.
37. **Silver I, Kim C, Mollanji R, Johnston M.** Cerebrospinal fluid outflow resistance in sheep: impact of blocking cerebrospinal fluid transport through the cribriform plate. *Neuropathol Appl Neurobiol* 28: 67–74, 2002.
38. **Sorensen P, Gjerris F, Schmidt J.** Resistance to CSF outflow in benign intracranial hypertension, (Pseudo-tumor Cerebri). In: *Outflow of Cerebrospinal Fluid*, edited by Gjerris F, Borgesen SE, and Sorensen PS. Copenhagen: Munksgaard, 1989.
39. **Tada T, Zhan H, Tanaka Y, Hongo K, Matsumoto K, Nakamura T.** Intraventricular administration of hepatocyte growth factor treats mouse communicating hydrocephalus induced by transforming growth factor beta1. *Neurobiol Dis* 21: 576–586, 2006.
40. **Welch K, Friedman V.** The cerebrospinal fluid valves. *Brain* 83: 454–469, 1960.
41. **Welch K, Pollay M.** Perfusion of particles through arachnoid villi of the monkey. *Am J Physiol* 201: 651–654, 1961.
42. **Zakharov A, Papaiconomou C, Djenic J, Midha R, Johnston M.** Lymphatic cerebrospinal fluid absorption pathways in neonatal sheep revealed by subarachnoid injection of Microfil. *Neuropathol Appl Neurobiol* 29: 563–573, 2003.
43. **Zakharov A, Papaiconomou C, Johnston M.** Lymphatic vessels gain access to cerebrospinal fluid through unique association with olfactory nerves. *Lymphat Res Biol* 2: 139–146, 2004.
44. **Zakharov A, Papaiconomou C, Koh L, Djenic J, Bozanovic-Sosic R, Johnston M.** Integrating the roles of extracranial lymphatics and intracranial veins in cerebrospinal fluid absorption in sheep. *Microvasc Res* 67: 96–104, 2004.